



Comment on “New probing techniques of radiative shocks”



Michel Busquet*

ARTEP, Inc. Ellicott City, MD 21042, USA

ARTICLE INFO

Article history:

Received 18 January 2012

Received in revised form

12 April 2012

Accepted 17 September 2012

Available online 25 October 2012

Keywords:

X ray lasers
radiative shock
opacities

ABSTRACT

In this comment, we discuss the possibility of imaging the radiative precursor of a strong shock with a 21.2 nm soft x-ray laser probe and we analyze the data presented in C.Stehlé et al “New probing techniques of radiative shocks”, (Optics Communications 285, 64, 2012) in order to derive some estimation of the achieved resolution. We show that the presented results are inconclusive for the existence of a radiative precursor. Furthermore, our best estimation of cold and warm Xenon VUV opacities tells that 21.2 nm backlighting would not be able to probe this radiative precursor.

© 2012 Elsevier B.V. All rights reserved.

1. Introduction

In C.Stehlé et al., 2011 [1] (named hereafter “paper I”), the authors present results obtained on the PALS facility for a Radiative Shock launched by a laser ablated piston in the line of previous similar experiments [2–5]. This time the authors used the unconverted laser ($\lambda=1.315\text{ }\mu\text{m}$) but at the same laser irradiance of 10^{14} W/cm^2 , not accounting for the suggested 25% off pointing error [6]. Some of these results were also presented, with images of better quality, in the proceeding of a PALS meeting [7] (name hereafter “paper II”). The shock is launched in a Xe-filled miniature shock tube ($0.4\text{ mm}\times 6\text{ mm}$) by a laser-ablated piston. The piston is a gold-coated plastic foil, where the plastic facing the laser converts the laser energy into piston velocity, using the so-called rocket effect. The gold layer acts as an inertia reservoir (the foil areal mass does not change during the observed times) and aims also to block hard x-rays created by the laser interaction process. However it may not stop suprathermal electrons created by resonant absorption (or x-rays created by them) that were suppressed in previous experiments by using the third harmonic ($\lambda=0.438\text{ }\mu\text{m}$). Hot spots and significant preheating of the gas may result. If the shock velocity is large enough and the preheat of the gas not too strong, a radiative precursor is launched by the shock.

The goal of the described experiment is to measure at the same time the position of the hydrodynamic shock (i.e. the density jump) and of the radiative precursor (a temperature wave, with no bulk density increase). Two diagnostics are presented. The first one is a

spatially resolved VUV absorption. The absorption spatial profile is obtained with an x-ray laser probe at $\lambda=21.2\text{ nm}$, thanks to a special target design derived from the one used in the previous experiment [8]. Since no measure of the achieved spatial resolution has been presented, the reader has to derive spatial resolution (along the tube axis, the pertinent one) from the published images [1,7]. Our estimation of the spatial resolution of the transmission curve is $0.4\pm 0.1\text{ mm}$ as the readers can infer from the following section. Paper I presents also time resolved measurement of the self-emission in the VUV and XUV range. From the geometry described in the paper, one can infer a 7 ns time resolution for one of the diodes, and 17 ns for the other one (see Section 3). Recorded profiles rather suggest a 15–20 ns resolution.

In the following sections, we discuss the possibility to image the precursor with a 21.2 nm XRL probe and we analyze the presented data to derive some estimation of the achieved resolution.

2. Analyzing VUV absorption profile

This absorption profile is obtained from a coherent VUV imaging using an astigmatic off-axis spherical mirror. The angle of incidence is unknown, it is probably between 0.2 and 0.5 rad. From the description given in paper I, the magnification is 8.2 and the focal length is 30 cm, therefore the image plane is located at $(1+8.2)\times 30\text{ cm}=276\text{ cm}$ from the mirror. Shielding of the self-emission of the target is obtained with a 0.5 mm diameter diaphragm located in the focal plane, therefore at 246 cm from the image plane, resulting in a very low aperture of $f/4920$ (Fig. 1). As the pinhole size is smaller than the object to be imaged, the different parts of the object (along the tube axis) are imaged by different parts of the mirror. Slope and position errors from the

* Tel.: +1 33683057232.

E-mail address: busquet@artepinc.com

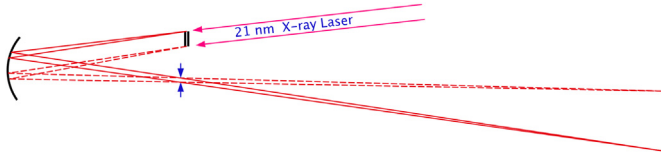


Fig. 1. Imaging system layout, here drawn for a magnification of 4, showing the shock tube to be imaged (drawn as a short thick line), the spherical off-axis imaging mirror, the apodizing diaphragm (blue arrows in this figure) and the image. Distances from object to mirror, from mirror to the 0.5 mm diaphragm (set at the focal spot of parallel rays), and from diaphragm to image plane, are deduced from the focal length and the magnifying ratio given in paper I (30 cm and 8.2). They are respectively 33.7 cm, 30 cm and 246 cm. The aperture of the optical system is then 0.05/246. Different positions of the mirror image different positions of the shock tube (imaging of each end is drawn with respect to plain line and dashes). (For interpretation of the references to color in this figure legend, the reader is referred to the web version of this article.)

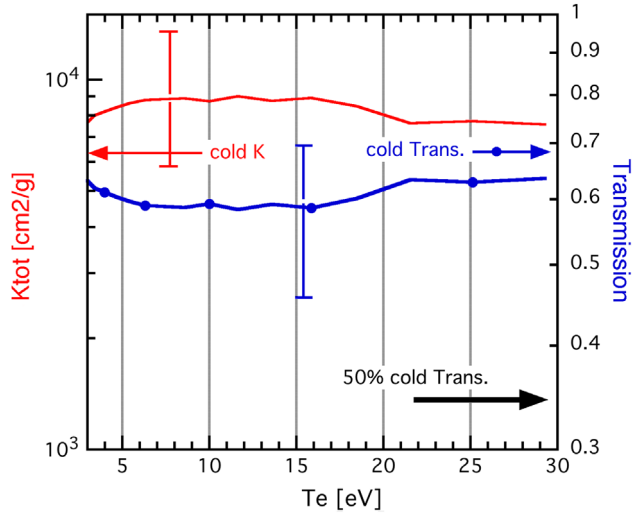


Fig. 2. Computed opacity at $\lambda=21.2$ nm of 0.3 bar Xenon and transmission of 0.4 mm slab vs. temperature. Low contrast with cold opacity and transmission (arrows) is found. Black thick arrow is drawn for 50% of the cold Xenon transmission. (For interpretation of the references to color in this figure legend, the reader is referred to the web version of this article.)

ideal curve of the reflecting surface result in a downgraded spatial resolution, in addition to the speckle pattern probably due to reflectivity variation of the multilayer coating, clearly seen in Fig. 6 of paper I and page 25 of paper II. Finally, because the mirror is off axis, tangential and sagittal focal lengths differ by 12–80 mm for angle of incidence of 0.2–0.5 rad, resulting in an out of focus blurring in one direction, of around 100–500 μm . Refraction by the strong gradient inherent to the shock should not downgrade the spatial resolution. Shock also might be non planar (at small scale) if the heating beam is not smoothed (the presence of a smoothing zone plate is not mentioned in paper I) and this would add to the blurring of the shock front. The penumbra zone (around $x=1.8$ mm in Fig. 7 of paper I, see also Fig. 7 of the present comment) has a 0.4 ± 0.1 mm extension [9] and is claimed by the authors to be a trace of the precursor, but can result from all the mentioned source of blurring along the shock propagation direction. Note that the decrease of transmission on the right (from 1–0.5 mm in Fig. 7 of paper I) may also be attributed to limited spatial resolution. With a good longitudinal resolution of the transmission curve, the shock would appear sharply, with a 10 times stiff increase in density ($Ni=Ne < Z >$ value derived from Fig. 5 of paper I).

Furthermore, we compute the Xenon opacity with the state-of-the-art atomic physics code STA [10] and we found that Xenon has

an almost constant opacity (Fig. 2) for temperatures from 3 to 30 eV and a density of 1.5 mg/cm^3 (i.e. pressure of 0.3 bar). By comparing different highly ranked opacity codes [11] we estimate a theoretical “uncertainty” of $\pm 30\%$, and much less for the relative variation with temperature. The whole precursor, if it exists, would then have a constant transmission of 0.6 ± 0.1 , which is very close (Fig. 3) to the cold Xenon transmission of 0.7 [12]. Therefore the 21.2 nm XRL probe would not be able to discriminate the precursor from the cold Xenon and would not give the observed 50% contrast (Fig. 7 of paper I) between the cold Xenon and the claimed-to-be-warm Xenon.

In summary, the large penumbra zone is more probably due to the insufficient quality of the imaging system, the deconvolution process, and/or the non-uniformity of piston velocity. High resolution would reveal the stiff density jump in the shock. We present in Fig. 4 the computed transmission obtained with a 0.5 mm spatial resolution and a model two steps absorption profile corresponding to first step the shocked gas and dense piston (less than 100 μm

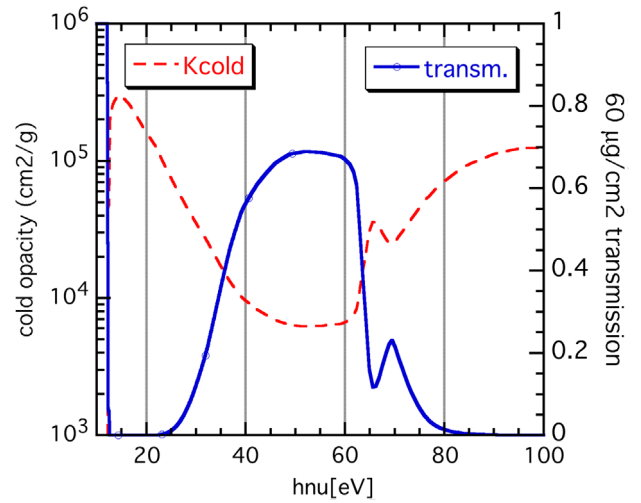


Fig. 3. 0.3 bar Xe cold opacity [11] vs. photon energy and transmission of 0.4 mm Xe gas at 0.3 bar.

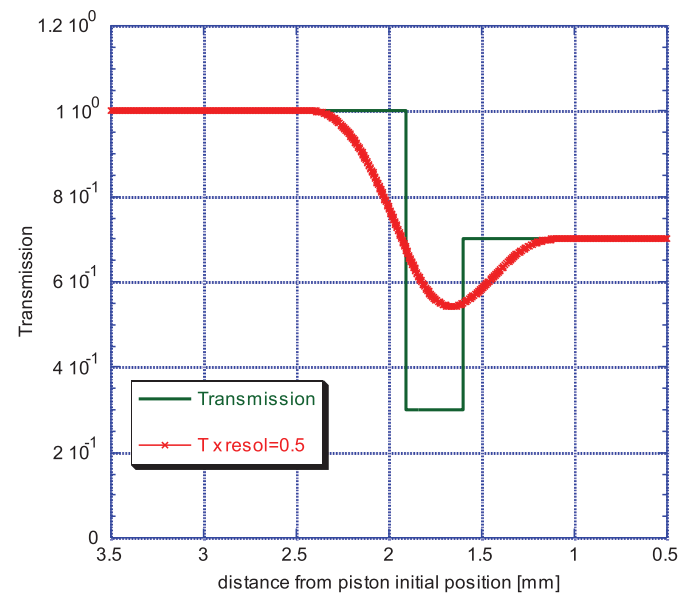


Fig. 4. Spatial transmission given by a simple shock (green, thin line) convolved with a 0.5 mm spatial resolution (red, thick line). (For interpretation of the references to color in this figure legend, the reader is referred to the web version of this article.)

Download English Version:

<https://daneshyari.com/en/article/1534956>

Download Persian Version:

<https://daneshyari.com/article/1534956>

[Daneshyari.com](https://daneshyari.com)